

Surface-reconstruction-enhanced solubility of N, P, As, and Sb in III-V semiconductors

S. B. Zhang and Alex Zunger

Citation: [Applied Physics Letters](#) **71**, 677 (1997); doi: 10.1063/1.119827

View online: <http://dx.doi.org/10.1063/1.119827>

View Table of Contents: <http://scitation.aip.org/content/aip/journal/apl/71/5?ver=pdfcov>

Published by the [AIP Publishing](#)

Articles you may be interested in

[Effects of surfactants Sb and Bi on the incorporation of zinc and carbon in III/V materials grown by organometallic vapor-phase epitaxy](#)

[J. Appl. Phys.](#) **100**, 044904 (2006); 10.1063/1.2227707

[Effects of surface nitridation during nitrogen plasma ignition on optical quality of GaInAsN grown by solid source molecular beam epitaxy](#)

[J. Appl. Phys.](#) **94**, 2662 (2003); 10.1063/1.1591413

[Influence of Sb, Bi, Tl, and B on the incorporation of N in GaAs](#)

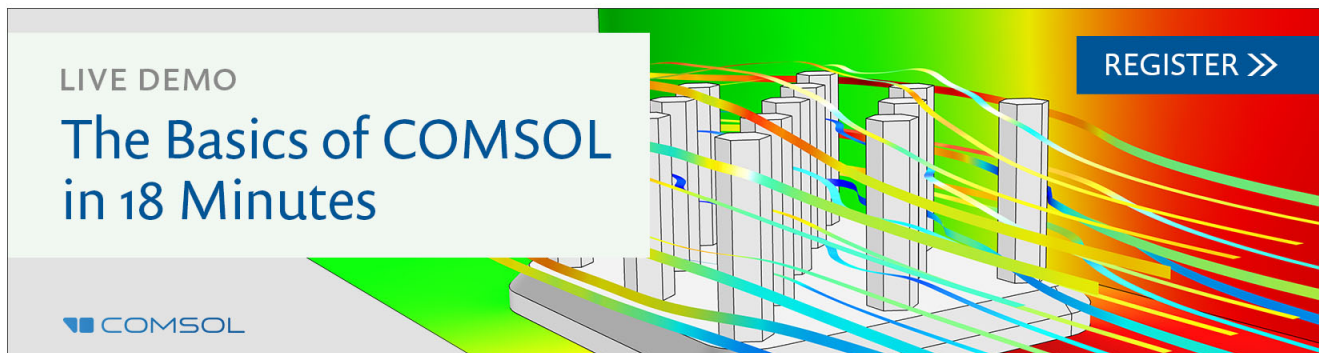
[J. Appl. Phys.](#) **91**, 3687 (2002); 10.1063/1.1450053

[High performance 1.3 \$\mu\text{m}\$ InGaAsN:Sb/GaAs quantum well lasers grown by molecular beam epitaxy](#)

[J. Vac. Sci. Technol. B](#) **18**, 1484 (2000); 10.1116/1.591409

[Effects of surface reconstruction on III-V semiconductor interface formation: The role of III/V composition](#)

[Appl. Phys. Lett.](#) **74**, 1704 (1999); 10.1063/1.123661

A promotional banner for COMSOL software. On the left, a white box contains the text 'LIVE DEMO' and 'The Basics of COMSOL in 18 Minutes'. The COMSOL logo is at the bottom left. The background features a 3D bar chart with colorful, flowing lines representing data or simulation results. A blue button with the text 'REGISTER >>' is located in the top right corner.

LIVE DEMO

The Basics of COMSOL in 18 Minutes

COMSOL

REGISTER >>

Surface-reconstruction-enhanced solubility of N, P, As, and Sb in III-V semiconductors

S. B. Zhang and Alex Zunger

National Renewable Energy Laboratory, Golden, Colorado 80401

(Received 21 March 1997; accepted for publication 29 May 1997)

We show that surface reconstructions may play an essential role in determining the equilibrium solubilities of N, P, As, and Sb in various III-V compounds. In particular, anion-anion dimerization of the (001)- $\beta 2(2 \times 4)$ surface can enhance the solubility of N near the surface in GaAs, GaP, and InP by five, three, and two orders of magnitudes, respectively, at 1000 K. With certain assumptions on the growth kinetics, this high concentration of N may be frozen in as the crystal grows. © 1997 American Institute of Physics. [S0003-6951(97)02731-9]

The solubility of nitrogen in III-V semiconductors is a subject of intensive study¹⁻³ as it holds the key to the success, as well as the limitations for making wide-band-gap GaNAs, GaNP, and InNP materials and devices. Recent vapor-phase growth experiments showed that 1% N can be incorporated into InP at $T=310-420$ °C,² 16% N in GaP at $T=500-610$ °C,³ and 1.6% in GaAs at $T=500$ °C.¹ However, a recent calculation,⁴ based on the valence-force-field model⁵ showed that the expected *bulk* solubility in these materials is far smaller, being 0.01%, 0.00001%, and 0.0000001% for InP, GaP, and GaAs, respectively, even at a much higher temperature of $T=727$ °C. Thus, the physical origin for the observed high N solubility in these materials is not understood.

In this context, it is important to note that nitrogen, being a first row element, differs from the other Group V elements in that its tetrahedral radius is only 0.75 Å, that is, 29% smaller than the next smallest Group V element, P. The low solubility $n(T)$ of small atoms substituted in *bulk* III-V compounds, stems from the large substitution energy ΔE_s , reflecting strain.⁶ However, it has recently been shown that the solubility of the small first row element, carbon, can be enhanced dramatically near the *surface* of Si.⁷ According to a recent calculation,⁸ the enhancement can reach five orders of magnitude relative to the bulk solubility. The dramatic increase of the solubility has two reasons: “surface strain relief” and “surface reconstruction” contributions. *First*, strain is more easily relieved near a surface than in the bulk, since near-surface atoms have more freedom to move. *Second*, surface reconstruction can relieve subsurface mismatch strain. This is illustrated in Fig. 1 that shows schematically an anion-stabilized (001) surface of a III-V compound, whose main feature is the occurrence of a *surface dimer bond*. In the bulk, two phosphorus atoms are *next* nearest neighbors, but at the surface, when dimerized they become *first* nearest neighbors. Consequently, the anion site directly *under* this strained dimer (labeled α) is under *compression*, while the anion site, above which there are no dimers (labeled β), feels *tension*. Of course, this subsurface selectivity exerted by surface dimers diminishes as one moves deeper into the film. However, this selectivity implies that if one places, sufficiently close to the surface, small solute atoms (e.g., N) at the α site, and larger (solvent) atoms at the β site, the overall strain energy ΔE_s will be reduced, so the solu-

bility $n(T)$ will rise. The mechanism of reconstruction-enhanced solubility is similar to that producing CuPt-like ordering in GaInP₂,^{9,10} where Ga (In) atoms occupy α -like (β -like) sites under the P-P dimer, except that unlike GaAs:N, here the concentration of the “solute atom” can reach 50%.

In this letter we will calculate the substitution energy $\Delta E_s^{(h)}(A:C:B)$ of an A atom by a B atom in the h -th subsurface layer of a binary AC(001) film. Our discussion follows the same spirit of Ref. 8. We will assume simplistically the same, geometric, 2×1 reconstruction for all III-V compounds, so as to illustrate generic surface effects versus bulk effects. Since, however, the real surface reconstruction modes of InP¹¹ differ from GaAs,¹² we expect that the calculated trends between different solvent semiconductors will be only qualitative. We will consider nine cases—GaAs:N, GaAs:P, GaAs:Sb, InP:N, InP:As, InP:Sb, GaP:N, GaP:As, and GaP:Sb, where the host material (solvent) is shown on the left, while the dopant (solute) is indicated on the right. We find that while in the *bulk*, the solvent-to-solute size mismatch tends to *increase* the substitution energy and *reduce* solubility, at the dimerized *surface*, size mismatch may actually *lower* the substitution energy near the surface and *enhance* solubility.

The substitution energy is modeled here by the valence force field approach. The impurity-host bond energy of

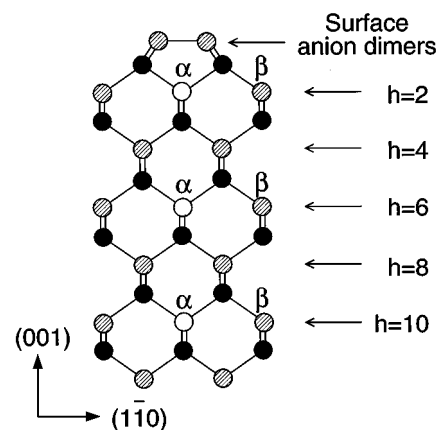


FIG. 1. Atomic structure of the dimerized (001)- 2×1 surface. The solid dots represent cations, while the open and hatched dots represent anions on the α and β sites, respectively.

TABLE I. Solubility of nitrogen (in cm^{-3}) in III-V compounds. Theoretical results represent the lower bounds to the solubilities at $T=727^\circ\text{C}$.

	GaAs	GaP	InP
^a Calc	Bulk $\sim 10^{14}$	$\sim 10^{16}$	$\sim 10^{19}$
This work	Bulk 10^{14}	2×10^{16}	5×10^{19}
	Surface 2×10^{19}	6×10^{19}	6×10^{21}
$\exp(T=310-610^\circ\text{C})$	3×10^{21b}	3×10^{22c}	2×10^{21d}

^aReference 4.

^bReference 1.

^cReference 3.

^dReference 2.

chemical origin is ignored. This is reasonable because (i) the chemical energy is not sensitive to height h and (ii) only the (small) second difference of the chemical energy enters the calculation of the equilibrium impurity concentration $n(T, h)$. For $X = n(T, h)/A \ll 1$, we have

$$n(T, h) = A e^{-\Delta E_s^{(h)}/kT}, \quad (1)$$

where A is the number of substitution sites, $\Delta E_s^{(h)} = E_{\text{strain}}^{(h)} + \Delta E_{\text{chem}} - (\mu_i - \mu_h)$ with $E_{\text{strain}}^{(h)}$ being the strain energy, ΔE_{chem} is the difference between the chemical energy of the impurity (i) and that of the host atom (h) being removed, and the μ 's are the chemical potentials. For simplicity, we consider here only the case of substituting impurity *molecules* into the host, e.g., substituting GaN molecules from a bulk GaN reservoir into GaAs, so the chemical potentials here are those of bulk GaN and bulk GaAs, respectively. Thus, $(\mu_i - \mu_h)$ is also a chemical energy difference between the impurity and the host molecules in their respective bulk, and $\delta\Delta E = \Delta E_{\text{chem}} - (\mu_i - \mu_h)$ is the second difference in chemical energy. First-principles linearized augmented plane wave calculation¹³ showed that $\Delta E_s^{\text{bulk}} = 1.9$ eV versus our strain-only energy of 1.8 eV for GaAs:N, thus $\delta\Delta E \sim 0.1$ eV. Since we neglect all other choices of the chemical potentials, only the *lower bound to the solubility limit* is obtained.

We minimize the $E_{\text{strain}}^{(h)}$ (consisting of bond bending and bond stretching) with respect to all atomic displacements, subject to the constraint that surface dimers are fixed. Contributions from fixed dimer atoms are omitted from the energy $E_{\text{strain}}^{(h)}$. Comparisons with first-principles results for GaInP alloy showed^{9,10} that this omission is a valid approximation. The dimer geometry for GaAs is obtained from self-consistent first-principles pseudopotential calculations¹⁴ and for GaP and InP, the dimer geometries are obtained by scaling the pseudopotential results for GaP and InP films coherently strained on a GaAs substrate.¹⁵ We use as input to the calculations the bulk bond lengths and bond bending/bond stretching force constants determined from first-principles pseudopotential calculations for GaAs, GaP, and InP.⁹ Because of the lack of pseudopotential force constants for GaN and InN, we used instead $\alpha_{\text{GaN}} = 81.01$ N/m and $\beta_{\text{GaN}} = 18.01$ N/m and $\alpha_{\text{InN}} = 70$ N/m and $\beta_{\text{InN}} = 8.06$ N/m, derived from measured elastic constants using the formula of Martin.¹⁶ This yields $\Delta E_s[\text{GaAs:N}] = 1.78$ eV/N, compared with $\Delta E_s = 1.70$ eV/N obtained with the recent local-density approximation derived force constants.¹⁷ Our calculated nitrogen *bulk* solubilities at $T=727^\circ\text{C}$ (Table I) are in reasonable agreement with the results of Ref. 4.

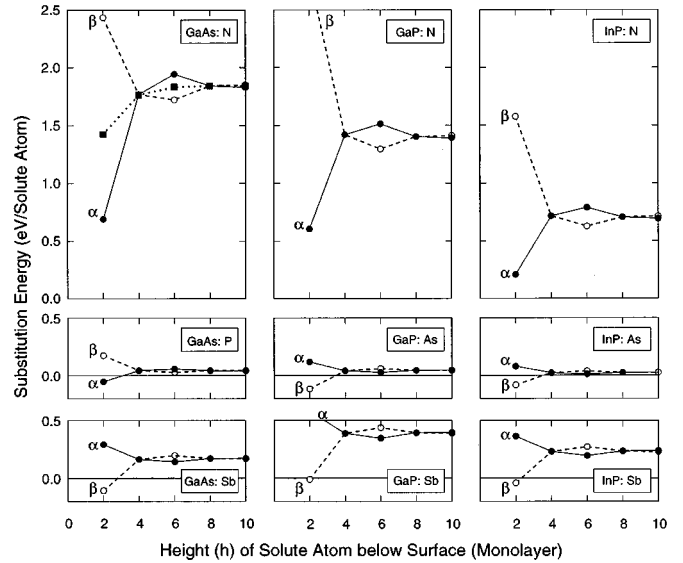


FIG. 2. Calculated substitution energies for Group V impurities in GaAs, GaP, and InP with a 4×4 surface cell. The filled dots denote energy for the α sites while the open dots denote energy for the β sites. For GaAs:N, results for an unreconstructed surface are also shown.

Figure 2 shows the calculated impurity substitution energies $\Delta E_s^{(h)}(X)$ as a function of its height h below the surface layer for N, P, As, and Sb impurities in GaAs, InP, and GaP, respectively. We have used in these calculations a 4×4 surface cell ($X=6.25\%$), so the nearest impurity-impurity distance is $2\sqrt{2}a_0$ where a_0 is the bulk lattice constant. We observed the following:

Trends with vertical and lateral impurity positions: The substitution energy is a strong function of the height h of the impurity below the surface: Taking GaAs:N as an example, at $h=2$, the N-to-As substitution energy (with nitrogen in the α site) is only 0.7 eV, while deeper in the film ($h=10$, which is bulklike) it is ~ 1.8 eV. There is thus a reduction of 1.1 eV if an N atom is brought from the bulk to the surface. There are two underlying physical reasons for this:⁸ strain relief near the surface and surface reconstruction. The former occurs since the surface is always free to relax along its normal. This lowers the substitution energy by a moderate 0.4 eV [see the dotted line in Fig. 2 giving $\Delta E_s^{(h)}$ for *unreconstructed* surfaces]. Surface reconstruction lowers the substitution energy by another 0.7 eV. Near the surface, the N atoms are also very site selective: for $h=2$, it takes 1.7 eV to move a nitrogen atom from the α site to the β site, hindering N diffusion across the dimer rows. There is a significant repulsion between the strain fields produced by different N atoms in a given subsurface layer h . This is shown in Fig. 3 illustrating the substitution energy $\Delta E_s^{(h=2)}(X)$ as a function of the lateral nitrogen concentration X in this layer. We see that the substitution energy per atom versus X fits well into a parabola, reaching the converged value of 0.64 eV as $X \rightarrow 0$.

Trends of different solute atoms in a given host: Considering the columns of Fig. 2, we see that the substitution energy is directly proportional to the size mismatch between the solute atoms (N, P, or Sb) and the host anion (for example, the As atoms in the first column in Fig. 2). The smaller the mismatch is, the smaller the substitution energy

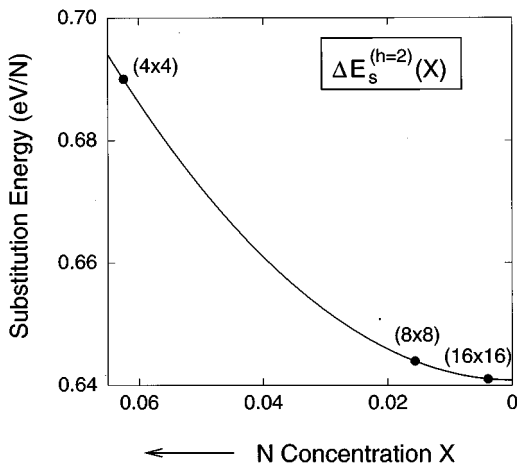


FIG. 3. The calculated substitution energies of nitrogen in GaAs at the $h = 2$ subsurface layer, as a function of N concentration X . The data were fitted to $\Delta E_s^{(h=2)} = 0.64 + 12.58X^2$ (eV) (i.e., the solid line).

is. Thus, the substitution energy is largest for N (-44% mismatch to As), next for Sb ($+15\%$ mismatch), and smallest for P (-7.5% mismatch).

α -to- β inversion for As and Sb: An interesting prediction is that when the solute atom is larger than the host anion (for example, in the case of Sb in GaAs), the solute atom prefers the β site over the α site.

Trends of a given solute in different hosts: Comparing ΔE_s along the rows in Fig. 2, e.g., the GaAs:N \rightarrow GaP:N \rightarrow InP:N sequence, we see that the substitution energy decreases monotonically. The fact that GaAs:N has the largest substitution energy while InP:N has the smallest substitution energy follows the lattice mismatch between the binaries: -20% between GaN/GaAs, -17% between GaN/GaP, and -15% between InN/InP. In GaP:N, a central N atom has four nearest-neighbor Ga atoms (the first shell) and twelve second-nearest-neighbor P atoms (the second shell). We find that (i) bond bending constitutes a major portion (75%) of the substitution energy, (ii) bond stretching energies come mostly from the first shell (67%), and (iii) bond bending energies are spread out into the host so the first shell accounts for $<1\%$. Thus, a large portion of the substitution energy involves the bending of non-N-containing Ga-P-Ga bonds (or In-P-In bonds for InP:N). Because $\beta_{\text{InP}} = 6.24$ N/m and $\beta_{\text{GaP}} = 10.45$ N/m, InP:N has much smaller strain energies than GaP:N (Fig. 2).

Spontaneous substitution: We see from Fig. 2 (rows 2 and 3) that for the solutes P, As, and Sb, the lowest substitution energies at $h = 2$ are all *negative*. This indicates that a size-mismatched solute atom near the surface may actually release more effectively the strain energy created by surface dimerization than the host atom itself.

The impurity concentration is calculated using Eq. (1). For concentration at the h -th layer, the coefficient A in Eq. (1) would be $N_A^{(001)} \times 3/4 \times 1/2$, where $N_A^{(001)} \sim 6 \times 10^{14} \text{ cm}^{-2}$ is the number of anion sites in a (001) layer, $3/4$ accounts for missing dimers on real $\beta 2(2 \times 4)$ surfaces, and $1/2$ signifies that only the α sites contribute. For volume concentration, we assume that at the experimental growth temperatures (500–900 K), impurity can freely enter the h

$= 2$ layer, but once buried (i.e., $h \geq 4$) it cannot diffuse out. Thus, $A = N_A \times 3/4 \times 1/2$, where $N_A = N_A^{(001)} \times (2/a_0) \sim 1.7 \times 10^{23} \text{ cm}^{-3}$ is the equivalent anion sites for impurity per volume, and $\Delta E_s^{(h)} = \Delta E_s^{(2)}$. The volume solubilities at $T = 727^\circ \text{C}$ are given in Table I. Compared with their respective bulk values, we obtain five, three, and two orders of magnitude surface enhancement of the nitrogen solubilities in GaAs, GaP, and InP.

To compare with the recent experimental data, we convert the observed solubilities into N formation energies using Eq. (1). This gives $\Delta E_s = 0.21$ eV (GaAs), 0.06 – 0.07 eV (GaP), and 0.18 – 0.22 eV (InP), while our calculated results are 0.7 eV (GaAs), 0.6 eV (GaP) and 0.2 eV (InP), respectively. It appears that the calculated formation energy for InP:N agrees with experiment while those for GaAs and GaP are too high. Thus, despite a 2×10^5 and 3×10^3 enhancement we predict relative low bulk solubilities for GaAs and GaP, experimental solubilities are still $\sim 10^2$ times higher. Two reasons can contribute. First, as we have pointed out, the calculated solubility limits are only the lower bound. For example, in Ga-containing III-V compounds nitrogen could prefer nonsubstitutional sites such as the interstitial sites. Second, the actual surface reconstruction patterns are strong functions of the growth conditions thus may also differ in GaAs, GaP, and InP, affecting N solubilities.

In conclusion, we showed that dimerization on the (001) surface may raise the solubility limits of N near the GaAs, GaP, and InP surfaces by orders of magnitudes. When the growth condition permits, the high N concentration may be frozen in as the crystal grows.

This work was supported by the Office of Energy Research, Division of Materials Science, U.S. Department of Energy, under Contract No. DE-AC36-83CH10093.

- ¹M. Weyers, M. Sato, and H. Ando, Jpn. J. Appl. Phys. 1 **31**, L853 (1992); M. Weyers and M. Sato, Appl. Phys. Lett. **62**, 1396 (1993).
- ²W. G. Bi and C. W. Tu, J. Appl. Phys. **80**, 1934 (1996).
- ³W. G. Bi and C. W. Tu, Appl. Phys. Lett. **69**, 3710 (1996).
- ⁴I. Ho and G. B. Stringfellow, MRS Symp. Proc. **449**, 871 (1997).
- ⁵P. N. Keating, Phys. Rev. **145**, 637 (1966).
- ⁶L. G. Ferreira, S. H. Wei, and A. Zunger, Phys. Rev. B **40**, 3197 (1989).
- ⁷H. J. Osten, M. Methfessel, G. Lippert, and H. Rucker, Phys. Rev. B **52**, 12 179 (1995).
- ⁸J. Tersoff, Phys. Rev. Lett. **74**, 5080 (1995).
- ⁹J. E. Bernard, S. Froyen, and A. Zunger, Phys. Rev. B **44**, 11 178 (1991).
- ¹⁰S. B. Zhang, S. Froyen, and A. Zunger, Appl. Phys. Lett. **67**, 3141 (1995).
- ¹¹C. D. MacPherson, R. A. Wolkow, C. E. J. Mitchell, and A. B. McLean, Phys. Rev. Lett. **77**, 691 (1996).
- ¹²M. D. Pashley, K. W. Haberen, W. Friday, J. M. Woodall, and P. D. Kirchner, Phys. Rev. Lett. **60**, 2176 (1988); D. K. Biegelsen, R. D. Briggans, J. E. Northrup, and L.-E. Swartz, Phys. Rev. B **41**, 5701 (1990).
- ¹³S.-H. Wei and A. Zunger, Phys. Rev. Lett. **76**, 664 (1996). See Ref. 9 in this letter where the miscibility gap temperature is $T_{\text{MG}} = 11\,024$ K corresponding to $\Delta E_s^{\text{bulk}} = 1.9$ eV.
- ¹⁴J. E. Northrup and S. Froyen, Phys. Rev. Lett. **71**, 2276 (1993); J. E. Northrup and S. Froyen, Phys. Rev. B **50**, 2015 (1994).
- ¹⁵S. Froyen and A. Zunger, Phys. Rev. B **53**, 4570 (1996).
- ¹⁶R. M. Martin, Phys. Rev. B **10**, 4005 (1970).
- ¹⁷K. Kim, W. R. Lambrecht, and S. Segall, Phys. Rev. B **53**, 16 310 (1996).